Monatsh Chem (2011) 142:219–224
DOI 10.1007/s00706-011-0450-5

ORIGINAL PAPER

Bismuth flux crystal growth of $RERh_6P_4$ (RE = Sc, Yb, Lu): new phosphides with a superstructure of the $LiCo_6P_4$ type

Ulrike Pfannenschmidt · Ute Ch. Rodewald · Rainer Pöttgen

Received: 11 November 2010 / Accepted: 29 January 2011 / Published online: 22 February 2011

Abstract The rhodium-rich phosphides $RERh_6P_4$ (RE = Sc, Yb, Lu) were synthesized from the constituent elements in bismuth fluxes and their structures were refined from X-ray single-crystal diffractometer data: $P\bar{3}$, $a = 6.968(2)$, $c = 3.666(2)$ Å, wR (F^2) = 0.0481, 895 F^2 for $ScRh_6P_4$; $a = 6.971(1)$, $c = 3.673(1)$ Å, wR (F^2) = 0.0614, 700 F^2 for $YbRh_6P_4$; $a = 6.971(2)$, $c = 3.682(1)$ Å, wR (F^2) = 0.0828, 722 F^2 for $LuRh_6P_4$ with 37 variables per refinement. All three crystals are twinned. The twinning and the structural relationship with the aristotype $LiCo_6P_4$, space group $P\bar{6}m2$ are discussed on the basis of a group–subgroup scheme. The $RERh_6P_4$ phosphides belong to the large number of metal-rich compounds with a metal-to-phosphorus ratio near 2:1. The isolated phosphorus atoms have trigonal prismatic metal coordination by RE and Rh atoms. The high rhodium content leads to a pronounced rhodium substructure (278–293 pm Rh–Rh in $ScRh_6P_4$). From a geometrical point of view, the $RERh_6P_4$ structures can be viewed as intergrowth variants of slightly distorted $ThCr_2Si_2$-related slabs as realized for KRh_2P_2.

Keywords Phosphide · Crystal chemistry · Metal flux

Introduction

Ternary phosphides $R_xRh_yP_z$ (R = alkali, alkaline earth, rare earth, or actinoid metal) have only scarcely been investigated. This is due to the high price and also the low reactivity of rhodium. So far, the phosphides RRh_2P_2 (R = K, Rb, Cs, Ca, Sr, Ba, La, Ce, Pr, Nd, Eu) [1–5] with $ThCr_2Si_2$- or $CaBe_2Ge_2$-type structure, $R_2Rh_{12}P_7$ (R = Sr, Zr, Nd, Gd, Tb, Dy, Ho, Er, Yb) [6–8], $R_6Rh_{30}P_{19}$ (R = Ca, Eu, Yb) [9], $RE_6Rh_{32}P_{21}$ (RE = La, Ce) [10], $(La, Ce)_{12}Rh_{30}P_{21}$ [11], $La_{18}Rh_{96}P_{51}$ [12], $U_6Rh_{20}P_{13}$ [13], $Sr_2Rh_7P_6$ [14], $Mg_4Rh_7P_6$ [15], and $MgRh_6P_4$ [16] have been synthesized and structurally characterized.

Preparation of these phosphides proceeds by different techniques. For a simple ceramic synthesis route, fine powders of the elements can be reacted in corundum or molybdenum crucibles at high temperature, followed by slow cooling rates. Such reactions often require repeated grinding and annealing cycles to obtain pure polycrystalline products. Well-shaped single crystals of most $R_xRh_yP_z$ phosphides were grown via lead fluxes [17]. The excess flux can easily be removed by oxidation through a mixture of glacial acetic acid and hydrogen peroxide (30%).

Extending our recent work on bismuth or lead flux growth of several $RE_xIr_yP_z$ phosphides (RE = rare earth element) [18–21], we also investigated the rhodium-containing systems. Herein we report on the trigonal phosphides $RERh_6P_4$ (RE = Sc, Yb, Lu) which crystallize with a superstructure of the $LiCo_6P_4$ type [22].

Results and discussion

Structure refinements

Careful analyses of the three diffractometer data sets revealed primitive hexagonal lattices and no systematic extinctions. In agreement with the energy-dispersive X-ray (EDX) analyses and the Guinier powder patterns we suggested isotypism with $LiCo_6P_4$ [22], space group $P\bar{6}m2$, a

U. Pfannenschmidt · U. Ch. Rodewald · R. Pöttgen (✉)
Institut für Anorganische und Analytische Chemie,
Westfälische Wilhelms-Universität Münster,
Corrensstrasse 30, 48149 Münster, Germany
e-mail: pottgen@uni-muenster.de

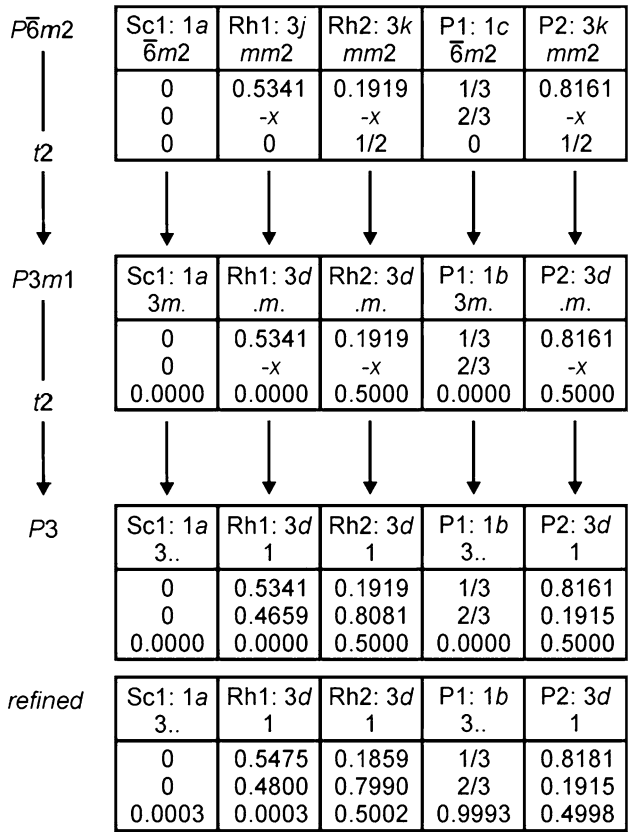

Fig. 1 Group–subgroup scheme in the *Bärnighausen* formalism [27–30] for the subcell and the superstructure of $ScRh_6P_4$. The indices for the *translationengleiche* symmetry reductions and the evolution of the atomic parameters are given

structure type which was also observed for the chemically related compounds α-UCr_6P_4 [23], $MgCo_6P_4$ [24], $MgRh_6P_4$, $MgRh_6As_4$, $CaRh_6As_4$, $SrRh_6As_4$, and $YbRh_6As_4$ [16]. The structure of the scandium compound was refined first. The positional parameters of $LiCo_6P_4$ [22] were taken as starting values and the structure was refined using SHELXL-97 [25, 26] (full-matrix least-squares on F^2) with anisotropic atomic displacement parameters for all sites. This refinement converged to $R_1 = 0.0678$ and $wR_2 = 0.1741$ with enhanced $U_{11} = U_{22}$ values for Rh1 and enhanced U_{33} for P2. Considering the high residual and the anisotropic displacements we assumed twinning and a symmetry reduction. Also the high standard deviation of the batch scale factor (BASF) value of 0.5(7) was indicative of a symmetry problem.

Inspection of the subgroups of $P\bar{6}m2$ led to the *Bärnighausen* tree [27–30] presented in Fig. 1. Subsequent refinement of the structure with Jana 2006 [31] in space group $P3$ (two *translationengleiche* symmetry reductions from $P\bar{6}m2$ via $P3m1$ to $P3$), assuming the twin matrix (−1 0 0, 1 1 0, 0 0 1) drastically drops the residuals to the values listed in Table 1. The $YbRh_6P_4$ and $LuRh_6P_4$ crystals showed the same twinning and were refined adequately. The final difference-Fourier synthesis revealed no significant residues. The refined atomic positions and the anisotropic displacement parameters are given in Tables 2 and 3. As an example we present the interatomic distances of $ScRh_6P_4$ in Table 4. Further information on the structure refinements is available in the "Experimental".

Crystal chemistry

The new rhodium-rich phosphides $RERh_6P_4$ (*RE* = Sc, Yb, Lu) belong to the large family of metal-rich compounds with a metal-to-phosphorus ratio near or equal to 2:1 with layered structures. Overviews on the rich crystal chemistry, the building principles, and the physical properties of these phosphides are given in diverse review articles [32–34]. One of the basic building principles of such metal-rich phosphides is the trigonal prismatic metal coordination of the phosphorus atoms. This is emphasized for $ScRh_6P_4$ in the left-hand part of Fig. 2. The building units drawn with thin and thick lines are shifted by approximately half the *c* translation period. The P1 atoms within the rhodium prisms are capped by three additional rhodium atoms on the rectangular sites, leading to coordination number nine, as typically observed for such structures. This is different for the P2 atoms. They are located in distorted trigonal prisms formed by four rhodium and two scandium atoms. Because of the propeller-like condensation motif of these trigonal prisms, only two of the rectangular faces are capped by additional rhodium atoms. Although this description is a purely geometrical one, it is well suited to describe and distinguish the large number of different structure types of metal-rich phosphides [32].

The shortest interatomic distances in the $ScRh_6P_4$ structure occur for Rh–P. They range from 228 to 258 pm. The shorter ones compare well with the sum of the covalent radii [35] of 235 pm, indicating substantial covalent Rh–P bonding, similar to $La_4Rh_8P_9$ (229–254 pm) [36] or $MgRh_6P_4$ (242–250 pm) [16]. Together, the rhodium and phosphorus atoms build up a three-dimensional $[Rh_6P_4]$ network which leaves hexagonal prismatic cages (6 Rh + 6 P atoms) for the scandium atoms (Fig. 2). As could be expected from the high rhodium content, within the $ScRh_6P_4$ structure we observe a broad range of Rh–Rh distances (278–293 pm). They are only slightly longer than in *fcc* rhodium (269 pm) [37]. Therefore, the Rh–Rh contacts also contribute to the stability of the $ScRh_6P_4$ structure. A cutout of the rhodium substructure is presented in Fig. 3.

$ScRh_6P_4$ is one of the metal-rich phosphides with a very simple structure; only 11 atoms per unit cell. The very complex structures within this family of compounds can often be described as intergrowth variants [32, 38] of

Table 1 Crystallographic data and structure refinement for $ScRh_6P_4$, $YbRh_6P_4$, and $LuRh_6P_4$, space group $P3$, $Z = 1$

Formula	$ScRh_6P_4$	$YbRh_6P_4$	$LuRh_6P_4$
Molar mass (g mol^{-1})	786.28	914.37	916.30
Lattice parameters (Å)	$a = 6.968(2)$	$a = 6.971(1)$	$a = 6.971(2)$
	$c = 3.666(2)$	$c = 3.673(1)$	$c = 3.682(1)$
Cell volume (Å^3)	$V = 154.2$ (2)	$V = 154.6(2)$	$V = 155.0(2)$
Density calc. (g cm^{-3})	8.47(1)	9.82(1)	9.82(1)
Crystal size (μm)	10 × 40 × 60	10 × 30 × 50	20 × 40 × 60
Detector distance (mm)	60	80	80
Exposure time (min)	3	3	3
ω range; increment (deg)	0–180, 1.0	0–180, 1.0	0–180, 1.0
Integr. param. A, B, EMS	12.8; 2.6; 0.012	13.0; 3.0; 0.012	12.8; 2.1; 0.013
$h\ k\ l$ range	±11; ±11; ±5	±10; ±10; ±5	±10; ±10; ±5
θ_{min}, θ_{max} (°)	3.4/34.8	3.4/31.8	3.4/31.8
Linear absorption coeff. (mm^{-1})	17.6	31.5	32.3
No. of reflections	4,652	3,779	3,843
R_{int}	0.0714	0.0820	0.1324
No. of independent reflections	895	700	722
Reflections used [$I \geq 3\sigma(I)$]	886	699	720
$F(000)$, e	351	400	401
R factors $R(F)/wR(F^2)$	0.0203/0.0481	0.0227/0.0614	0.0392/0.0828
No. of refined parameters	37	37	37
Goodness-of-fit	1.52	1.68	1.34
Twin ratio	15(2):23(1):31(1):31(1)	25(3):34(2):24(2):17(2)	26(2):24(1):25(1):25(1)
Extinction coefficient	718(19)	440(15)	116(10)
Diff. Fourier residues (e Å^{-3})	−0.80, +0.68	−1.72, +2.10	−2.50, +2.25

Table 2 Atom positions and equivalent isotropic displacement parameters (Å^2) for $ScRh_6P_4$, $YbRh_6P_4$, and $LuRh_6P_4$

Atom	Wyckoff position	x	y	z	U_{eq}
$ScRh_6P_4$					
Sc	1*a*	0	0	0.0004*	0.0173(3)
Rh1	3*d*	0.5475(1)	0.4800(1)	0.0003(1)	0.0183(2)
Rh2	3*d*	0.1859(1)	0.7990(1)	0.5002(1)	0.0168(2)
P1	1*b*	1/3	2/3	0.9993(7)	0.0197(4)
P2	3*d*	0.8181(4)	0.1915(3)	0.4998(4)	0.0201(4)
$YbRh_6P_4$					
Yb	1*a*	0	0	0.00002*	0.0084(2)
Rh1	3*d*	0.5476(3)	0.4797(3)	0.994(2)	0.0091(4)
Rh2	3*d*	0.1878(3)	0.7960(2)	0.4927(19)	0.0071(4)
P1	1*b*	1/3	2/3	0.999(10)	0.0069(9)
P2	3*d*	0.8163(7)	0.1930(7)	0.501(7)	0.0070(12)
$LuRh_6P_4$					
Lu	1*a*	0	0	0.0689*	0.0155(2)
Rh1	3*d*	0.5365(6)	0.4679(5)	0.0634(17)	0.0140(7)
Rh2	3*d*	0.1971(6)	0.8032(5)	0.5594(9)	0.0128(7)
P1	1*b*	1/3	2/3	0.083(3)	0.0120(10)
P2	3*d*	0.802(2)	0.186(2)	0.580(3)	0.013(2)

* The z parameters of the *RE* sites were fixed during the refinement

simpler structure types. This is also possible for $ScRh_6P_4$. As emphasized at the right-hand part of Fig. 2, $ScRh_6P_4$ can be described as an intergrowth variant of slightly distorted $ThCr_2Si_2$-related slabs. Such an arrangement is known for KRh_2P_2 [5]. This classification scheme has successfully been applied to various metal-rich iridium phosphides [18–21].

Finally we draw back to the superstructure formation. So far, this structural arrangement has been observed for $LiCo_6P_4$ [22], α-UCr_6P_4 [23], $MgCo_6P_4$ [24], $MgRh_6P_4$, $MgRh_6As_4$, $CaRh_6As_4$, $SrRh_6As_4$, and $YbRh_6As_4$ [16]. All these phosphides and arsenides have been described with the higher symmetric hexagonal space group. A critical inspection of the displacement parameters of these compounds shows (1) enhanced equivalent isotropic parameters for Cr1 and P2 of α-UCr_6P_4 [23] and (2) enhanced U_{33} values for Co2 and P2 of $LiCo_6P_4$ [22]. It is interesting to note that preliminary X-ray film data of $ZrCr_6P_4$ [39] indicated a doubling of the subcell c axis. Most likely a second superstructure exists for the family of 1–6–4 phosphides. A detailed structural investigation on $ZrCr_6P_4$ and a reinvestigation of $LiCo_6P_4$ are in progress. Most likely the superstructure formation is a geometrical effect. This hypothesis, however, can only be verified when all 1–6–4 structures have been refined.

Table 3 Anisotropic displacement parameters (Å^2) for $ScRh_6P_4$, $YbRh_6P_4$, and $LuRh_6P_4$

Atom	U_{11}	U_{22}	U_{33}	U_{12}	U_{13}	U_{23}
$ScRh_6P_4$						
Sc	0.0185(5)	U_{11}	0.0147(5)	0.0093(2)	0	0
Rh1	0.0179(2)	0.0189(2)	0.0199(2)	0.0105(2)	0.00007(19)	0.0001(2)
Rh2	0.0157(2)	0.0158(2)	0.0192(2)	0.0081(1)	0.00009(17)	−0.00006(19)
P1	0.0186(6)	U_{11}	0.0218(7)	0.0093(3)	0	0
P2	0.0208(6)	0.0169(5)	0.0208(5)	0.0080(4)	0.0000(5)	0.0002(4)
$YbRh_6P_4$						
Yb	0.0089(2)	U_{11}	0.0073(3)	0.0044(1)	0	0
Rh1	0.0100(6)	0.0091(4)	0.0105(5)	0.0065(3)	−0.0003(15)	−0.0005(15)
Rh2	0.0063(5)	0.0058(4)	0.0091(6)	0.0030(3)	0.0015(12)	−0.0017(12)
P1	0.0062(9)	U_{11}	0.0083(18)	0.0031(5)	0	0
P2	0.0051(12)	0.0069(13)	0.008(2)	0.0019(12)	0.002(5)	−0.001(4)
$LuRh_6P_4$						
Lu	0.0173(3)	U_{11}	0.0119(3)	0.0086(2)	0	0
Rh1	0.0249(13)	0.0069(9)	0.0127(3)	0.0097(3)	0.006(2)	0.001(2)
Rh2	0.0147(10)	0.0121(11)	0.0116(5)	0.0066(3)	−0.004(2)	0.001(2)
P1	0.0145(11)	U_{11}	0.007(2)	0.0072(6)	0	0
P2	0.013(4)	0.010(3)	0.013(2)	0.0028(16)	0.014(4)	0.010(4)

Coefficients U_{ij} of the anisotropic displacement factor tensor of the atoms are defined by: $-2\pi^2[(ha^*)^2U_{11} + \cdots + 2hka^*b^*U_{12}]$

Table 4 Interatomic distances (Å) for $ScRh_6P_4$

Sc1			Rh2		
3	P2	2.904(2)	1	P2	2.280(2)
3	P2	2.906(2)	1	P2	2.311(3)
3	Rh2	2.968(1)	1	P1	2.491(3)
3	Rh2	2.969(1)	1	P1	2.495(3)
3	Rh1	3.413(1)	2	Rh1	2.815(2)
3	Rh1	3.603(1)	2	Rh1	2.836(2)
2	Sc1	3.666(1)	2	Rh2	2.926(1)
Rh1			1	Sc1	2.968(1)
1	P2	2.418(3)	1	Sc1	2.969(1)
1	P1	2.421(3)	P1		
1	P2	2.421(1)	3	Rh1	2.421(1)
1	P2	2.573(3)	3	Rh2	2.491(3)
1	P2	2.576(3)	3	Rh2	2.495(3)
2	Rh1	2.784(1)	P2		
2	Rh2	2.815(2)	1	Rh2	2.280(2)
2	Rh2	2.836(2)	1	Rh2	2.311(3)
			1	Rh1	2.418(3)
			1	Rh1	2.421(3)
			1	Rh1	2.573(3)
			1	Rh1	2.576(3)
			1	Sc1	2.904(3)
			1	Sc1	2.906(3)

All distances of the first coordination spheres are listed

Experimental

Synthesis

Single crystals of the three metal-rich phosphides were prepared by the bismuth flux technique [17]. Starting materials were pieces of scandium, ytterbium, and lutetium (Smart Elements, >99.9%), rhodium powder (Heraeus, >99.9%), red phosphorus (Hoechst, Knapsack, ultrapure), and bismuth shots (ABCR GmbH, 99.99%). Pieces of scandium, ytterbium, lutetium, rhodium powder, red phosphorus, and bismuth shots were mixed in molar ratios of 1:2:2:30 (Sc/Rh/P/Bi), 1:2:2:60 (Yb/Rh/P/Bi), and 3:2:2:30 (Lu/Rh/P/Bi) and sealed in evacuated silica tubes. The tubes were placed in a muffle furnace and first heated to 770 K at a rate of 20 K/h and kept at that temperature for 24 h. Subsequently the temperature was raised to 1,320 K at a rate of 50 K/h, kept at that temperature for 100 h, followed by slow cooling to 970 K at a rate of 2 K/h and further to 570 K at a rate of 4 K/h. The samples were quenched on air and the excess bismuth flux was slowly dissolved with a 1:1 molar mixture of glacial acetic acid (VWR International) and H_2O_2 (ACROS 35%). The resulting samples were washed with demineralised water. The reaction products consisted of partially intergrown pillar-shaped crystals with metallic lustre. By-products (which remained after the oxidative dissolution of the flux) were the binary rhodium phosphides Rh_2P and RhP_2.

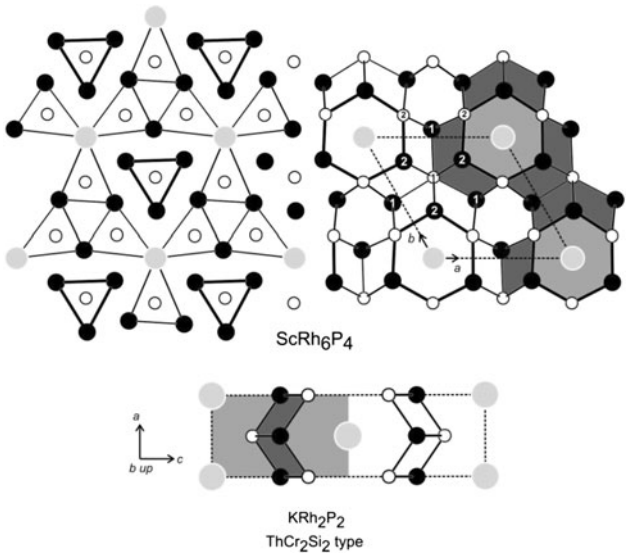

Fig. 2 Projection of the $ScRh_6P_4$ structure onto the *xy* plane. All atoms lie on mirror planes at $y \approx 0$ (*thin lines*) and $y \approx 1/2$ (*thick lines*). Scandium, rhodium, and phosphorus atoms are drawn as *medium grey*, *filled*, and *open circles*, respectively. The three-dimensional $[Rh_6P_4]$ network is emphasized at the *right-hand part* of the drawing and atom designations are given within the unit cell. The intergrowth character of $ThCr_2Si_2$ (KRh_2P_2)-related slabs is highlighted. The *left-hand part* of the drawing emphasizes the trigonal prismatic coordination of the phosphorus atoms. For details see text

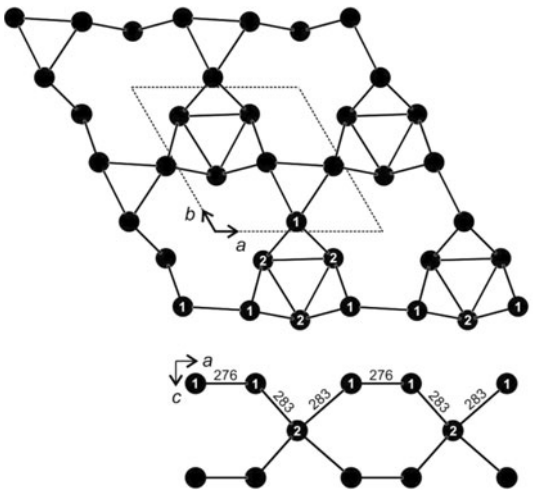

Fig. 3 *Top* the rhodium substructure of $ScRh_6P_4$ as a projection onto the *xy* plane. *Bottom* cutout of the rhodium substructure in *xz* projection. Atom designations and relevant interatomic distances are given

Scanning electron microscopy

Semiquantitative EDX analyses of single crystals investigated on the diffractometer and the bulk samples were carried out with a Zeiss EVO MA10 scanning electron microscope with Sc, YbF_3, LuF_3, Rh, GaP, and Bi as

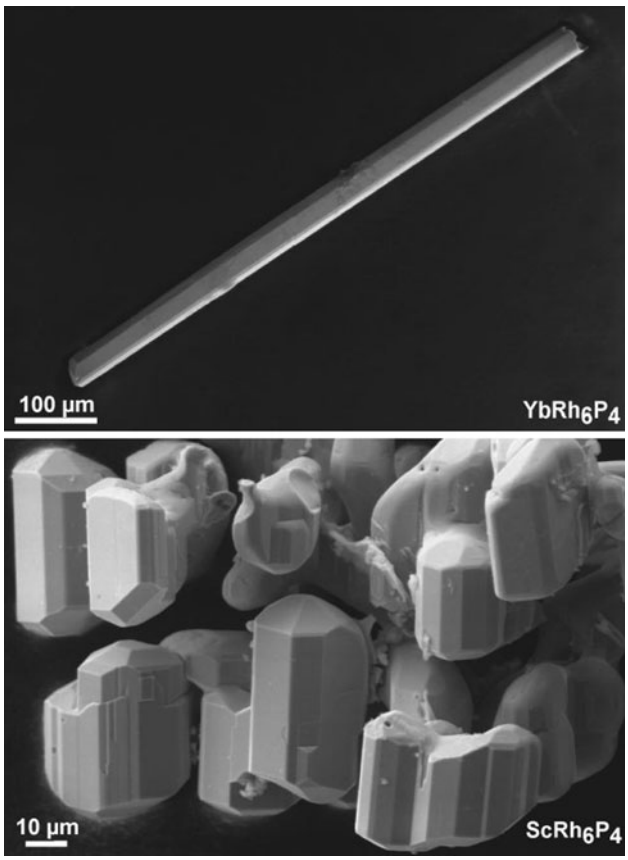

Fig. 4 Scanning electron micrographs of an $YbRh_6P_4$ rod (*top*) and intergrown blocks of $ScRh_6P_4$ (*bottom*)

standards. The experimentally observed compositions of 9 ± 2 at% *RE*: 55 ± 2 at% Rh: 36 ± 2 at% P were close to the ideal one (9.1:54.5:36.4). There was no hint of bismuth incorporation into the crystals, in agreement with the single-crystal X-ray data. However, some crystals showed small surface contamination with traces of undissolved bismuth. The $YbRh_6P_4$ and $LuRh_6P_4$ crystals formed as thin rods, whereas $ScRh_6P_4$ forms compact intergrown blocks (Fig. 4).

X-ray diffraction data

The flux grown samples were characterized by X-ray powder diffraction using a Guinier camera equipped with an image plate system (Fujifilm, BAS-1800) using Cu $K\alpha_1$ radiation and α-quartz ($a = 4.9130$, $c = 5.4046$ Å) as an internal standard. The trigonal lattice parameters were deduced from least-squares refinements of the powder data. To ensure correct indexing, the experimental patterns were compared with calculated ones [40] using the positional parameters obtained from the structure refinements.

Pillar-shaped crystal fragments of $ScRh_6P_4$, $YbRh_6P_4$, and $LuRh_6P_4$ were separated from the flux-grown sample

by mechanical fragmentation. The pillars were glued to quartz fibres using beeswax and were characterized by Laue photographs on a Buerger camera (white molybdenum radiation, image plate technique, Fujifilm, BAS-1800) to check their suitability for an intensity data collection. The data sets were collected at room temperature by use of an IPDS II diffractometer (graphite monochromatized Mo Kα radiation; oscillation mode). Numerical absorption corrections were applied to the data sets. All relevant crystallographic data and details of the data collections and evaluations are listed in Table 1.

Further information on the structure refinements may be obtained from: Fachinformationszentrum Karlsruhe, D-76344 Eggenstein-Leopoldshafen (Germany), by quoting the Registry Nos. CSD–422333 ($ScRh_6P_4$), CSD–422334 ($YbRh_6P_4$), and CSD–422335 ($LuRh_6P_4$).

Acknowledgments This work was financially supported by the Deutsche Forschungsgemeinschaft.

References

1. Czybulka A, Noack M, Schuster H-U (1992) Z Anorg Allg Chem 609:122
2. Wurth A, Johrendt D, Mewis A, Huhnt C, Michels G, Roepke M, Schlabitz W (1997) Z Anorg Allg Chem 623:1418
3. Wenz P, Schuster H-U (1984) Z Naturforsch 39b:1816
4. Madar R, Chaudouet P, Senateur JP, Zemni S, Tranqui D (1987) J Less-Common Met 133:303
5. Rózsa S, Schuster H-U (1981) Z Naturforsch 36b:1668
6. Wurth A, Keimes V, Johrendt D, Mewis A (2001) Z Anorg Allg Chem 627:2183
7. Pivan J-Y, Guérin R, Sergent M (1984) C R Acad Sci Ser II 299:533
8. Pivan JY, Guérin R, Sergent M (1985) J Less-Common Met 107:249
9. Wurth A, Löhken A, Mewis A (2002) Z Anorg Allg Chem 628:661
10. Pivan J-Y, Guérin R, Pena O, Padiou J, Sergent M (1988) Mater Res Bull 23:513
11. Pivan JY, Guérin R (1986) J Less-Common Met 120:247
12. Pivan J-Y, Guérin R, Sergent M (1987) J Solid State Chem 68:11
13. Ghetta V, Chaudouet P, Madar R, Senateur JP, Lambert-Andron B (1987) Mater Res Bull 22:483
14. Wurth A, Mewis A (1999) Z Anorg Allg Chem 625:1486
15. Wurth A, Löhken A, Mewis A (2001) Z Anorg Allg Chem 627:1213
16. Wurth A, Mewis A (1999) Z Anorg Allg Chem 625:449
17. Kanatzidis MG, Pöttgen R, Jeitschko W (2005) Angew Chem 117:7156
18. Pfannenschmidt U, Rodewald UC, Pöttgen R (2010) Z Anorg Allg Chem 636:314
19. Pfannenschmidt U, Rodewald UC, Pöttgen R (2010) Z Kristallogr 225:280
20. Pfannenschmidt U, Rodewald UC, Pöttgen R (2011) Z Kristallogr 13 (in press)
21. Pfannenschmidt U, Rodewald UC, Pöttgen R (2011) Z Naturforsch 66b:7
22. Buschmann R, Schuster H-U (1991) Z Naturforsch 46b:699
23. Jeitschko W, Brink R (1992) Z Naturforsch 47b:192
24. Hellmann A, Mewis A (2001) Z Anorg Allg Chem 627:1357
25. Sheldrick GM (1997) SHELXL-97, program for cystal structure refinement. University of Göttingen
26. Sheldrick GM (2008) Acta Crystallogr A64:112
27. Bärnighausen H (1980) Commun Math Chem 9:139
28. Bärnighausen H, Müller U (1996) Symmetriebeziehungen zwischen den Raumgruppen als Hilfsmittel zur straffen Darstellung von Strukturzusammenhängen in der Kristallchemie. Universität Karlsruhe und Universität/GH Kassel
29. Müller U (2004) Z Anorg Allg Chem 630:1519
30. Wondratschek H, Müller U (2010) International tables for crystallography, vol A1: symmetry relations between space groups, 2nd edn. Wiley, Chichester
31. Petricek V, Dusek M, Palatinus L (2006) Structure determination software programs. Institute of Physics, University of Prague, Prague (Czech Republic)
32. Kuz'ma Yu, Chykhrij S (1996) Phosphides. In: Gschneidner KA Jr, Eyring L (eds) Handbook on the physics and chemistry of rare earths, vol 23. Elsevier, Amsterdam, chap 156, p 285
33. Chykhrij SI (1999) Pol J Chem 73:1595
34. Pöttgen R, Hönle W, von Schnering HG (2005) Phosphides: solid state chemistry. In: King RB (ed) Encyclopedia of inorganic chemistry, vol VII, 2nd edn. Wiley, New York, p 4255
35. Emsley J (1999) The elements. Oxford University Press, Oxford
36. Pfannenschmidt U, Johrendt D, Behrends F, Eckert H, Eul M, Pöttgen R (2011) Inorg Chem (in press)
37. Donohue J (1974) The structures of the elements. Wiley, New York
38. Parthé E, Chabot B, Cenzual K (1985) Chimia 39:164
39. Brink R (1989) Strukturchemische Untersuchungen von Phosphiden des Urans mit Chrom und Molybdän. Dissertation, Universität Münster
40. Yvon K, Jeitschko W, Parthé E (1977) J Appl Crystallogr 10:73